



Study of conjugate conduction–laminar film condensation for a vertical plate fin

HAN-TAW CHEN, ZEN LAN and TZUNG-I WANG

Department of Mechanical Engineering, National Cheng Kung University, Tainan, Taiwan 701,
 Republic of China

(Received 6 January 1993 and in final form 25 November 1993)

INTRODUCTION

THE USE of condensing fins is very extensive in the application of heat exchange. In investigating heat-transfer characteristics of a condensing fin, the conjugate problem with the condensate boundary layer and heat conduction in the fin must be considered. Conjugate heat transfer from fins has received considerable attention in recent years [1–5]. However, a few investigators studied the laminar boundary layer analysis of film condensation on a vertical plate fin in the presence of the interfacial shear at the condensate–vapor interface.

Due to the work of Nusselt, considerable work has been done on laminar film condensation from isothermal surfaces. However, only a few investigators [6–12] studied laminar film condensation on a vertical fin. Patankar and Sparrow [6] solved the coupled problem of condensation on an extended surface. Lienhard and Dhir [7] investigated the case of laminar film condensation without the interfacial resistance on various geometries for which similar solutions can be obtained. However, they did not simultaneously solve boundary layer equations in two phases and heat conduction in the fin. Acharya *et al.* [8] proposed two simpler methods to calculate the fin efficiency of laminar film condensation on various fin shapes. Sarma *et al.* [9] studied laminar film condensation on a vertical plate fin of variable thickness. In these previous works [6–12] not only the shear at the liquid–vapor interface was assumed to be negligible but also the Nusselt model was used.

Yang [13] considered laminar film condensation on non-isothermal plates in a brief note. He developed a complex scheme for solving boundary layer equations and found some deviations from the Nusselt–Rohsenow results. The present study is concerned with laminar film condensation on a vertical plate fin in the presence of the shear force at the liquid–vapor interface. In addition, effects of various parameters, such as Pr , Ja and Nc , on the heat transfer rate are also taken into account. Due to the non-linearity and close coupling, all the equations must simultaneously be solved. The 1-D heat conduction equation in the fin and boundary layer equations in two phases are respectively solved by using the central finite-difference approximation and the local non-similarity method [14]. The main purpose of the present study is to investigate the difference between the present results and those obtained from the Nusselt model [10–12].

ANALYSIS

A schematic diagram of the physical model with the coordinate system is shown in Fig. 1. A vertical plate fin of thickness $2t$ and length L ($L \gg 2t$) is attached to a wall at its temperature T_0 and is placed in the pure vapor at its saturation temperature T_s . T_s is assumed to exceed the tem-

perature at the fin base T_0 . Thus condensation occurs on the fin and, in steady state, a continuous laminar film of condensate flows downward along it due to the action of gravity g . Along the liquid–vapor interface, the vapor velocity tangent to the interface is the same as that of the liquid if there is no slip. The vapor velocity approaches zero at some distance away from the interface. Consequently, there simultaneously exist both liquid and vapor boundary layers. Assume that the condensate on the fin forms a laminar, non-rippling film. In addition, the assumptions made in the analysis for the isothermal case [15] are also applied in the present study.

Liquid

$$\frac{\partial u}{\partial x} + \frac{\partial v}{\partial y} = 0, \quad (1)$$

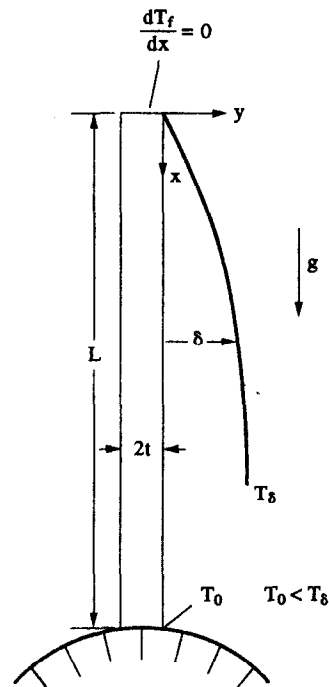


FIG. 1. Physical configuration of the present study.

NOMENCLATURE

E fin efficiency
 f, F reduced stream function for condensate and vapor
 g $\partial f/\partial \xi$, or acceleration of gravity
 G $\partial F/\partial \xi$
 \hat{h} dimensionless local heat transfer coefficient
 h_{fg} latent heat of condensate
 Ja Jakob number, $c_p(T_s - T_0)/h_{fg}$
 k_i, k_L thermal conductivity of the condensate and fin
 L fin length
 Nc conduction-film condensation parameter, $Lk_L c_L/k_f t$
 Pr Prandtl number
 Q overall fin heat transfer rate
 q local natural-convection heat flux
 R $[(\rho\mu)_L/(\rho\mu)_v]^{1/2}$
 T, T_i temperature of the condensate and fin
 T_0 temperature at the fin base

t half thickness of the fin
 u, v velocity components
 x, y coordinates.

Greek symbols

α thermal diffusivity of the condensate
 β volumetric coefficient of thermal expansion
 δ film thickness
 η pseudo-similarity variable
 θ, θ_f dimensionless temperature of the condensate and fin
 ν kinematic viscosity
 ξ dimensionless variable
 ϕ $\partial \theta/\partial \xi$
 ψ stream function.

Subscripts

L condensation film
 v vapor phase.

$$u \frac{\partial u}{\partial x} + v \frac{\partial u}{\partial y} = g \left(1 - \frac{\rho_v}{\rho_L} \right) + \nu_L \frac{\partial^2 u}{\partial y^2}, \quad (2)$$

$$u \frac{\partial T}{\partial x} + v \frac{\partial T}{\partial y} = \alpha_L \frac{\partial^2 T}{\partial y^2}. \quad (3)$$

The variation of fluid properties is neglected, and the viscous dissipation term is omitted from the energy equation since it is negligibly small. All the fluid properties are those of the condensate except ρ_v , which is the density of the vapor.

Vapor

Next, turning to the vapor, due to the assumption of the saturation condition, the vapor temperature is essentially constant. Thus the energy equation need not be considered, and only the continuity and momentum equations remain.

$$\frac{\partial u_v}{\partial x} + \frac{\partial v_v}{\partial y} = 0, \quad (4)$$

$$u_v \frac{\partial u_v}{\partial x} + v_v \frac{\partial u_v}{\partial y} = \nu_v \frac{\partial^2 u_v}{\partial y^2}. \quad (5)$$

The boundary conditions for this problem are:

$$u = v = 0 \quad T = T_w(x) \quad \text{at} \quad y = 0, \quad (6a)$$

$$u_v \rightarrow 0 \quad \text{at} \quad y \rightarrow \infty, \quad (6b)$$

$$u = 0 \quad \text{at} \quad x = 0 \quad y \geq 0. \quad (6c)$$

Interface matching. It is clear that the velocity, mass transfer, shear force and temperature along the interface must be matched in both the liquid and vapor phases [15]. These compatibility requirements are given as:

$$u = u_v, \\ \dot{m} = \rho_L \left(u \frac{d\delta}{dx} - v \right) = \left(\rho u \frac{d\delta}{dx} - \rho v \right),$$

$$\left(\mu \frac{\partial u}{\partial y} \right)_L = \left(\mu \frac{\partial u}{\partial y} \right)_v,$$

and

$$T = T_s \quad \text{at} \quad y = \delta. \quad (7)$$

The 1-D heat conduction equation for a thin fin with its negligible tip leakage of heat is given as

$$\frac{d^2 T_f(x)}{dx^2} = \frac{h(x)}{k_f t} [T_f(x) - T_s], \quad (8)$$

where k_f is the thermal conductivity of the fin. The equation is subjected to the following boundary conditions as:

$$T_f = T_0 \quad \text{at} \quad x = 0, \quad (9a)$$

$$\frac{dT_f}{dx} = 0 \quad \text{at} \quad x = L. \quad (9b)$$

Local non-similarity transformation

The continuity equation (1) can be satisfied by introducing a stream function ψ_L such that $u = \partial \psi_L / \partial y$ and $v = -\partial \psi_L / \partial x$. The remaining partial differential equations can be transformed into the corresponding ordinary differential equations by the following dimensionless parameters. To do this, a dimensionless coordinate ξ is introduced as:

$$\xi = x/L. \quad (10)$$

The dimensionless constants c_L and c_v , pseudo-similarity variables η_L and η_v , reduced stream functions f and F and dimensionless temperature θ are defined, respectively, as:

Liquid layer:

$$c_L = \left[\frac{g(\rho_L - \rho_v)L^3}{4\nu_L^2 \rho_L} \right]^{1/4} \quad \eta_L = \frac{c_L y}{L\xi^{1/4}},$$

$$\psi_L = 4\nu_L c_L \xi^{3/4} f(\xi, \eta_L) \quad \theta = \frac{T - T_s}{T_0 - T_s}; \quad (11)$$

Vapor layer:

$$c_v = \left[\frac{L^3}{4\nu_v^2} \right]^{1/4} \quad \eta_v = \frac{c_v y}{L\xi^{1/4}} \quad \psi_v = 4\nu_v c_v \xi^{3/4} F(\xi, \eta_v). \quad (12)$$

Velocity components in the condensate film can be expressed in terms of the new variables as:

$$u = 4\nu_L c_L^2 \xi^{1/2} f'/L, \quad (13)$$

$$v = \nu_L c_L \xi^{-1/4} L^{-1} \left(\eta_L f' - 3f - 4\xi \frac{\partial f}{\partial \xi} \right). \quad (14)$$

With these dimensionless variables in equations (10)–(12), the momentum and energy equations for the liquid and vapor layers are then transformed into a set of the dimensionless

forms :

$$f''' + 3ff'' - 2(f')^2 + 1 = 4\zeta \left(f' \frac{\partial f'}{\partial \zeta} - f'' \frac{\partial f}{\partial \zeta} \right), \quad (15)$$

$$Pr^{-1}\theta'' + 3f\theta' = 4\zeta \left(f' \frac{\partial \theta}{\partial \zeta} - \theta' \frac{\partial f}{\partial \zeta} \right), \quad (16)$$

$$F''' + 3FF'' - 2(F')^2 = 4\zeta \left(F' \frac{\partial F}{\partial \zeta} - F'' \frac{\partial F}{\partial \zeta} \right). \quad (17)$$

The boundary conditions (6) and (7) can be written as :

$$f = f' = 0 \quad \theta = \theta_w(\zeta) \quad \text{at} \quad \eta = 0, \quad (18a)$$

$$f' = F' \quad Rf'' = F'' \quad R \left(3f + 4\zeta \frac{\partial f}{\partial \zeta} \right) = 3F + 4\zeta \frac{\partial F}{\partial \zeta},$$

$$\theta = 0 \quad \text{at} \quad \eta_L = \eta_{L\delta}, \quad (18b)$$

$$F' \rightarrow 0 \quad \text{at} \quad \eta \rightarrow \infty, \quad (18c)$$

where $\theta_w = (T_w - T_s)/(T_0 - T_s)$, $R = [(\rho\mu)_l/(\rho\mu)_v]^{1/2}$ and $Pr = \nu_l/\alpha_l$. The primes denote differentiation with respect to η_l for the liquid layer and to η_v for the vapor layer. It is evident that the momentum equation is independent of the energy equation. Thus momentum equations are solved separately provided certain compatibility conditions at the interface can be satisfied. Moreover, the solution of the momentum equation depends on R and the dimensionless thickness of the condensate film $\eta_{L\delta}$. The effect of R on the heat transfer rate was always neglected for condensing fins in previous works [6–12]. However, its effect will be considered in the present study.

It is evident that the system of equations (15)–(18) constitutes a mathematical form for laminar film condensation of a saturated vapor on the vertical plate fin under the gravitational action. Once $\theta_w(\zeta)$ is specified, the system of equations can be solved.

The thermal coupling between the conduction equation and the energy equation in the liquid layer is expressed by the requirement that the temperature and heat flux must be continuous at the fin–liquid interface. These conditions are given as :

$$T_l(x) = T_w(x), \quad (19)$$

$$-k_l \left. \frac{\partial T}{\partial y} \right|_{y=0} = h(x)[T_l(x) - T_s]. \quad (20)$$

Using the dimensionless variable $\theta_l = (T_l - T_s)/(T_0 - T_s)$ can yield the dimensionless forms of equations (8) and (9) as :

$$\frac{d^2\theta_l(\zeta)}{d\zeta^2} = Nch(\zeta)\theta_l(\zeta), \quad (21)$$

and

$$\frac{d\theta_l}{d\zeta} = 0 \quad \text{at} \quad \zeta = 0, \quad (22a)$$

$$\theta_l = 1 \quad \text{at} \quad \zeta = 1, \quad (22b)$$

where Nc is denoted as the conjugate conduction–film condensation parameter and is given as :

$$Nc = \frac{L}{k_l t} k_1 c_1. \quad (23)$$

The dimensionless heat transfer coefficient \hat{h} is defined as :

$$\hat{h}(\zeta) = \frac{hL}{k_l c_1} = - \left[\frac{1}{\zeta} \right]^4 \left[\frac{\partial \theta}{\partial \eta} \right]_{\eta=0}. \quad (24)$$

The liquid film thickness δ (and hence $\eta_{L\delta}$) is not known *a priori* and is one of the results of the present study. As stated by Koh *et al.* [15], $\eta_{L\delta}$ can be obtained from an energy balance at the liquid–vapor interface. The relation at this interface is

given as :

$$k_l \left. \frac{\partial T}{\partial y} \right|_{y=\delta} = \dot{m} h_{fg}. \quad (25)$$

Substituting the dimensionless parameters shown in equation (11) into equation (7) in conjunction with the definition of the stream function ψ_L yields :

$$\dot{m} = \rho_l c_{1v} L^{-1} \zeta^{-1/4} \left(3f + 4\zeta \frac{\partial f}{\partial \zeta} \right). \quad (26)$$

Thus the dimensionless form of equation (25) can be written as :

$$Ja = -Pr \left[\left(3f + 4\zeta \frac{\partial f}{\partial \zeta} \right) / \theta' \right]_{\eta=\eta_{L\delta}}, \quad (27)$$

where Ja is the Jakob number and is defined as $Ja = c_{pv}(T_s - T_0)/h_{fg}$. As stated by Koh *et al.* [15], there exists a unique relation between $\eta_{L\delta}$ and Ja for a given value of Pr , Nc and R . Thus $\eta_{L\delta}$ should carefully be chosen to yield a physical significant variation in (Ja, R, Nc, Pr) .

NUMERICAL METHOD

Equations (15)–(18) are solved approximately by the two-equation model of the local non-similarity method [14]. To this end, the following three functions for generating the two-equation model are introduced as :

$$g(\zeta, \eta) = \partial f / \partial \zeta \quad G(\zeta, \eta) = \partial F / \partial \zeta \quad \varphi(\zeta, \eta) = \partial \theta / \partial \zeta. \quad (28)$$

Owing to these definitions in equation (28), equations (15)–(17) can be transformed into six ordinary differential equations. Three additional differential equations are obtained by differentiating equations (15)–(17) with respect to ζ . To close the system of equations at the second-order level, terms involving $\partial g / \partial \zeta$, $\partial G / \partial \zeta$ and $\partial \varphi / \partial \zeta$, etc., are ignored. Under this simplifying assumption, the whole set can be treated as a coupled system of ordinary differential equations, parameterized in ζ :

$$f''' + 3ff'' - 2(f')^2 + 1 = 4\zeta(f'g' - f''g), \quad (29)$$

$$Pr^{-1}\theta'' + 3f\theta' = 4\zeta(f'\varphi - \theta'g), \quad (30)$$

$$F''' + 3FF'' - 2(F')^2 = 4\zeta(F'G' - F''G), \quad (31)$$

$$g''' + 3fg'' + 7g'f'' - 8f'g' = 4\zeta(g'g' - g''g), \quad (32)$$

$$Pr^{-1}\varphi'' + 3f\varphi' + 7g\theta' - 4f'\varphi = 4\zeta(g'\varphi - \varphi'g), \quad (33)$$

$$G''' + 3FG'' + 7GF'' - 8F'G' = 4\zeta(G'G' - G''G). \quad (34)$$

The approximate boundary conditions are required for solving the three additional equations (32)–(34). Under the circumstances, the whole set of boundary conditions is given by

$$f = f' = g = g' = 0 \quad \text{at} \quad \eta_L = 0, \quad (35a)$$

$$\theta = \theta_l = \theta_w(\zeta) \quad \varphi = \partial \theta_l / \partial \zeta \quad \text{at} \quad \eta_L = 0, \quad (35b)$$

$$f' = F' \quad Rf'' = F'' \quad 3f + 4\zeta G = R(3f + 4\zeta g) \quad g' = G'$$

$$Rg'' = G'' \quad G = Rg \quad Ja = -Pr[(3f + 4\zeta g)/\theta']$$

$$\text{at} \quad \eta_L = \eta_{L\delta}, \quad (35c)$$

$$F' = G' = 0 \quad \text{at} \quad \eta_v \rightarrow \infty. \quad (35d)$$

It is evident that equations (29), (31), (32) and (34) can be solved independently, and then equations (30) and (33) are solved by using results of “ f ” and “ g ” through equations (29) and (32). One hundred fin grid points are used in the present study. The grid point deployment is uniform. It can be found from equations (21) and (24) that the location at the fin tip ($\zeta = 0$) is a singular point. To overcome this difficulty in the numerical treatment for this singular point, approximate values of $\partial \theta_l / \partial \zeta$ and θ_l at $\zeta = \Delta \zeta$ are given.

respectively, as:

$$\frac{d\theta_f}{d\xi} \Big|_{\xi=\Lambda_\xi} = \frac{4}{3} Nc \left[-\frac{\partial\theta}{\partial\eta} \right]_{\eta=0} (\Delta\xi)^3, \quad (36)$$

and

$$\theta_f \Big|_{\xi=\Lambda_\xi} = \frac{16}{21} Nc \left[-\frac{\partial\theta}{\partial\eta} \right]_{\eta=0} (\Delta\xi)^7 + \theta_f \Big|_{\xi=0}. \quad (37)$$

The discretized form of equation (21) in the interval, $\Delta\xi \leq \xi \leq 1$, using the central finite-difference algorithm, is

$$\frac{\theta_{f,i+1} - 2\theta_{f,i} + \theta_{f,i-1}}{\Delta\xi^2} = Nc \hat{h}_i \theta_{f,i} \quad i = 1, 2, \dots, 99, \quad (38)$$

where $\theta_{f,0} = \theta_f(0)$ is an initially guessed value. $\theta_{f,100} = \theta_f(1) = 1$.

Distributions of f , F and θ at a specific position ξ , depend only on $\eta_{L,\delta}$ for the given value of Pr , Nc , Ja and R . The iterative procedures of the present method are followed for the solution of equations (21), (22), (27) and (29)–(35).

- (1) We give a predictive value of $\theta_f(0)$. Then, for the given value of Pr , Ja , R and $\eta_{L,\delta}$, the boundary layer equations (29)–(35) can be solved by using the fourth-order Runge–Kutta method in conjunction with the Nachtsheim–Swigert iteration scheme [18] to fulfil boundary conditions at the edge of the vapor layer. If the energy balance equation at the liquid–vapor interface (27) is not satisfied, a new guess for $\eta_{L,\delta}$ will again be made. The entire calculation is repeated until equation (27) is satisfied. Values of $\hat{h}_i(\Delta\xi)$ and $\eta_{L,\delta}(\Delta\xi)$ can be obtained from these computational procedures.
- (2) Values of $\hat{h}_i(\Delta\xi)$ and $\theta_f(\Delta\xi)$ obtained from step (1) are used as input data for determining results at the next location. The results of $d\theta_f/d\xi$ and θ_f at $\xi = 2\Delta\xi$ can be obtained from equation (38). However, \hat{h} at $\xi = 2\Delta\xi$ must be determined from boundary layer equations. These computational processes are continued until $\xi = 1$.
- (3) Steps (1) and (2) are repeated until $|\theta_{f,cont}(\xi = 1) - 1| < 10^{-3}$.

The local heat flux q along the condensing fin can be expressed as:

$$q(x) = -k_L \frac{\partial T}{\partial y} \Big|_{y=0} = h(x)[T_f(x) - T_s]. \quad (39)$$

Substituting equations (11) and (24) into equation (39) yields the dimensionless form of $q(x)$ as:

$$\hat{q}(\xi) = \frac{qL}{k_L c_L (T_0 - T_s)} = - \left[\frac{1}{\xi} \right]^{1.4} \left[\frac{\partial\theta}{\partial\eta} \right]_{\eta=0}. \quad (40)$$

The numerical values of the overall fin heat transfer rate $Q(x)$ can be obtained by integrating the local heat flux $q(x)$ over the condensing fin. However, all of the heat lost by the fin must be conducted into the fin base at $x = L$. Thus $Q(x)$ can be written as:

$$Q(x) = -2k_f t \frac{dT_f}{dx} \Big|_{x=L} = 2k_L \int_0^1 \left(\frac{\partial T}{\partial y} \right)_{y=0} dy. \quad (41)$$

The dimensionless form of equation (41) is:

$$\hat{Q} = \frac{Q}{k_L (T_s - T_0) c_L} = \frac{2}{Nc} \left[\frac{d\theta_f}{d\xi} \right]_{\xi=1}. \quad (42)$$

Assume that the fin efficiency is defined as the ratio of the actual condensation taking place on the fin to the heat transfer rate estimated from the classical Nusselt analysis for isothermal conditions of the surface maintained at its base temperature [9]. This implies that the fin efficiency E can be expressed as:

$$E = -k_{fL} \frac{dT_f}{dx} \Big|_{x=L} / \left[h_{iso} (T_s - T_0) L \right]. \quad (43)$$

The classical Nusselt analysis for a vertical isothermal surface gives the relation of the heat transfer coefficient at the isothermal condition h_{iso} as:

$$h_{iso} = (4k_L c_L / 3L) / (Pr/Ja)^{1/4}. \quad (44)$$

The substitution of equations (42) and (44) into equation (43) gives:

$$E = 0.375 \hat{Q} / (Pr/Ja)^{1/4}. \quad (45)$$

RESULTS AND DISCUSSION

Figure 2 shows that the effect of Nc on the dimensionless temperature distribution of the fin for $Pr = 2$, $R = 100$ and $Ja = 0.1, 0.008$. It is evident that the present results have some deviations from those obtained by using the Nusselt model [11, 12]. The difference of the temperature distribution between them increases with increasing Nc . It can be seen that the dimensionless temperature at the fin tip tends to the saturation temperature T_s with increasing Nc or decreasing Ja . At the same time, the larger the value of Nc , the steeper the dimensionless temperature gradient at the fin base. However, the fin efficiency E increases with decreasing Nc or increasing Ja , as shown in Fig. 3. Examining Fig. 3 and equation (45) indicates that the overall heat transfer rate \hat{Q} also decreases with increasing Nc because the fin becomes more non-isothermal. It may be noted that $Nc = 0$ implies an infinite thermal conductivity of the fin. An increase in Nc indicates an increase in k_L/k_f or L/t . The Jakob number Ja is a relative measure of the degree of subcooling experienced by the liquid film. Thus it can be concluded from the definition of Nc and Ja that the present numerical results are correct. Figure 3 also shows that the Nusselt model overpredicts the fin efficiency, and the difference of E between the present results and those obtained by the Nusselt model increases with decreasing Ja or increasing Nc . The maximum difference of E is about 14.8%.

The effect of the interfacial shear on velocity profiles at the fin base and the difference of f'' between the present results and those obtained by the Nusselt model [11, 12] are shown in Fig. 4. It is found that the velocity profile of the vapor layer shows a rapid decrease in magnitude for large values of R and is almost a vertical jump for values of R greater than 500. However, the effect of R on the velocity profile in the condensate can be neglected for the present study. It can also be observed that the maximum difference of f'' at the liquid–vapor interface between the two models is about 27% and the simple theory using the Nusselt model underpredicts the dimensionless condensate film thickness and the condensate velocity. It can be concluded from Figs. 2–4 that the application of the Nusselt model to the condensing fin has some deficiencies for larger Nc values.

The effects of Pr and Ja on the dimensionless local heat transfer coefficient \hat{h} are respectively shown in Figs. 5 and 6. Figure 5 shows that decreasing the value of Pr tends to decrease \hat{h} for a fixed value of R , Ja and Nc . This indicates that the inertia force tends to lower the heat transfer rate for a small Pr value. It can be seen from ref. [15] that an increase in Ja will thicken the condensate film thickness. Based on the assumption of the local heat transfer coefficient in the problem of laminar film condensation, increasing Ja can cause a substantial reduction of the heat transfer coefficient, as shown in Fig. 6.

CONCLUSIONS

The problem of conjugate conduction–laminar film condensation of the pure saturated vapor on a vertical plate fin

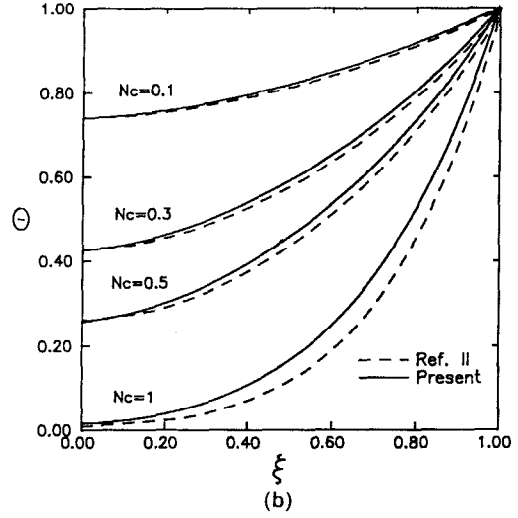
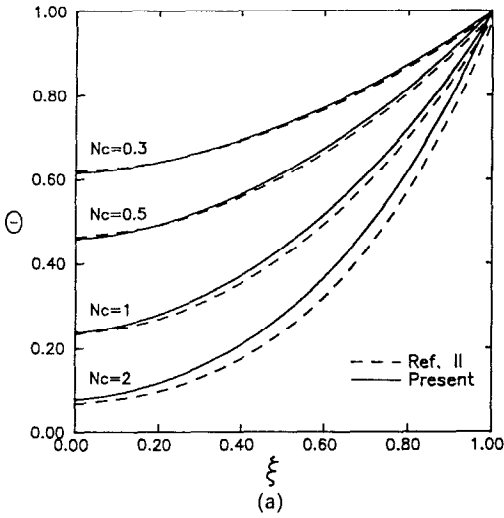


FIG. 2.(a) Effect of N_c on the temperature distribution of the fin for $Ja = 0.1$, $Pr = 2$ and $R = 100$.
 (b) Effect of N_c on the temperature distribution of the fin for $Ja = 0.008$, $Pr = 2$ and $R = 100$.

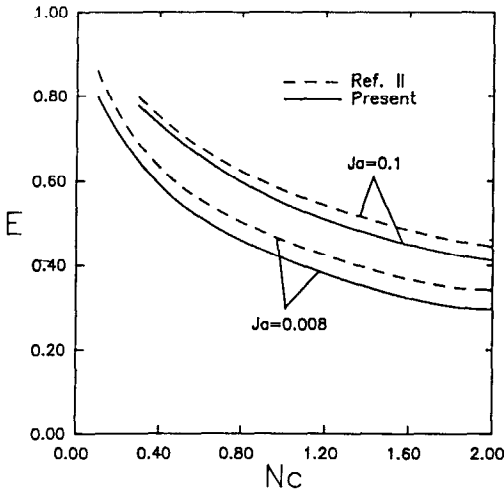


FIG. 3. Variation of the fin efficiency with N_c for $Pr = 2$, $R = 100$ and $Ja = 0.008, 0.1$.

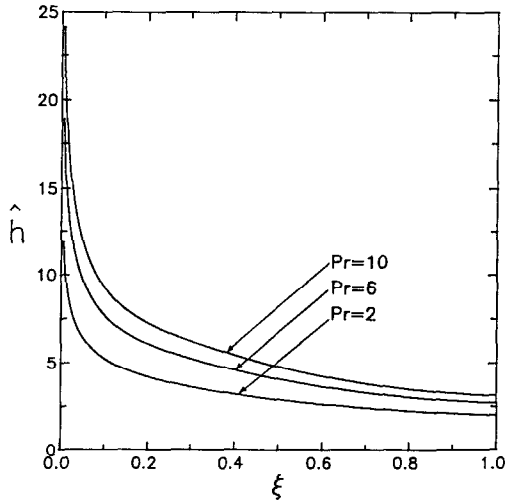


FIG. 5. Effect of Pr on the dimensionless local heat transfer coefficient for $R = 100$, $Ja = 0.2$ and $N_c = 2$.

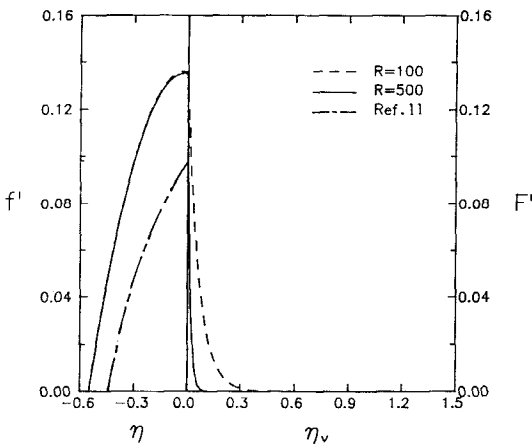


FIG. 4. Velocity profiles at the fin base for $Pr = 2$, $Ja = 0.2$, $N_c = 2$ and various R values.

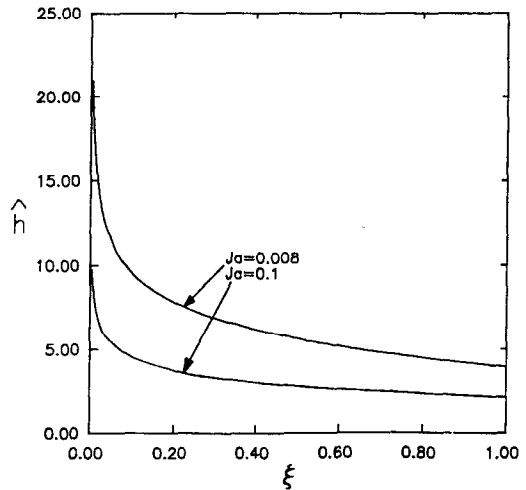


FIG. 6. Effect of Ja on the dimensionless local heat transfer coefficient for $Pr = 2$, $R = 100$ and $N_c = 1$.

has successfully been studied. A simple and efficient numerical method is proposed for its solution. The present results show that R ranging from 100 to 500 has a negligible effect on the velocity profile of the condensate. However, the obvious deviation of the velocity profile between the present results and those obtained from the Nusselt model can be observed. In addition, the simple theory using the Nusselt model overpredicts the fin efficiency, and underpredicts the dimensionless film thickness and the dimensionless temperature distribution of the fin. The difference of the fin efficiency between the two models is increased with increasing Nc or decreasing Ja . Thus it can be concluded that the application of the Nusselt model to the condensing fin may have some deficiencies for determining some physical results. A further extension of the present numerical scheme to other physical problems, such as the problem of the conjugate film condensation on one side of a vertical wall and natural convection on the other side, will be investigated in the future. The effect of the wavy action on such problems will be considered during subsequent development of the present analysis.

REFERENCES

1. E. M. Sparrow and S. Acharya, A natural convection fin with a solution-determined nonmonotonically varying heat transfer coefficient, *ASME J. Heat Transfer* **103**, 218–225 (1981).
2. B. Sunden, Conjugate mixed convection heat transfer from a vertical rectangular fin, *Int. Comm. Heat Mass Transfer* **10**, 267–276 (1983).
3. C. K. Chen and M. J. Huang, Heat transfer analysis for conjugate free convection–conduction in a vertical plate fin, *J. Chinese Institute Engr* **7**, 151–158 (1984).
4. V. K. Garg and K. Velusamy, Heat transfer characteristics for a plate fin, *ASME J. Heat Transfer* **108**, 224–226 (1986).
5. H. T. Chen and L. C. Fang, Simple computational method for conjugate conduction–convection along a vertical plate fin, *Engng Anal.* **10**, 93–98 (1992).
6. S. V. Patankar and E. M. Sparrow, Condensation on an extended surface, *ASME J. Heat Transfer* **101**, 434–440 (1979).
7. J. H. Lienhard and V. K. Dhir, Laminar film condensation on non-isothermal and arbitrary heat flux surfaces and on fins, *ASME J. Heat Transfer* **96**, 197–203 (1974).
8. S. Acharya, K. G. Braud and A. Attar, Calculation of fin efficiency for condensing fins, *Int. J. Heat Fluid Flow* **7**, 96–98 (1986).
9. P. K. Sarma, S. P. Chary and V. D. Rao, Condensation on a vertical plate fin of variable thickness, *Int. J. Heat Mass Transfer* **31**, 1941–1944 (1988).
10. W. K. Nader, Extended surface heat transfer condensation, Paper CS-5, *Sixth International Heat Transfer Conference* **2**, Toronto, Canada, pp. 407–412 (1978).
11. L. C. Burmeister, Vertical fin efficiency with film condensation, *ASME J. Heat Transfer* **104**, 391–393 (1982).
12. C. K. Chen and H. T. Chen, Study on laminar film condensation heat transfer onto fin, *J. CSME* **2**, 57–64 (1981).
13. K. T. Yang, Laminar film condensation on a vertical nonisothermal plate, *ASME J. Appl. Mech.* **88**, 203–205 (1966).
14. E. M. Sparrow and H. S. Yu, Local nonsimilarity thermal boundary-layer solutions, *ASME J. Heat Transfer* **93**, 328–334 (1971).
15. J. C. Y. Koh, E. M. Sparrow and J. P. Hartnett, The two phase boundary layer in laminar film condensation, *Int. J. Heat Mass Transfer* **2**, 69–82 (1961).
16. H. R. Nagera and M. A. Tirunaarayanan, Laminar film condensation from nonisothermal vertical flat plates, *Chem. Engng Sci.* **25**, 1073–1079 (1970).
17. E. M. Sparrow and S. H. Lin, Condensation heat transfer in the presence of a noncondensable gas, *ASME J. Heat Transfer* **C86**, 430–436 (1964).
18. J. A. Adams and D. F. Rogers, *Computer-Aided Heat Transfer Analysis*. McGraw-Hill, New York (1973).